Feature Extraction and Fusion for Automatic Target Recognition Based ISAR Images

SAIDI MOHAMED NABIL[1,2]
TOUMI ABDELMALEK[1]
KHENCHAF ALI[1]
ABOUTAJDINE DRISS[2]
HOELTZENER BRIGITTE[1]

[1] Laboratory E3I2-EA3876 ENSIETA, Brest,France
(Saidimo,Toumiab,Ali.Khenchaf,brigitte.hoeltzener)@ensieta.fr
[2] GSCM-LRIT, Faculty of Sciences,
Mohammed V University, Rabat, Morocco
Aboutaj@fsr.ac.ma

Abstract. This paper presents aircraft target recognition (ATR) system using Inverse Synthetic Aperture Radar (ISAR). The methodology used to design the complete processing chain from the acquisition step to the recognition (classification) step is based on the artificial intelligence approach. This process is known as Knowledge Discovery from Data (KDD) which we have adapted to radar target recognition system. We propose a new method for target shape extraction from ISAR images based on the combination of a modified SUSAN Algorithm and Variational of Level Set. To guarantee the invariance in translation and rotation of the extracted shape, the moment invariants and Fourier descriptors are used. In the second part of this work, We have investigated the impact of the information fusion on our recognition system. Therefore, three combination strategies: probability theory, majority vote and belief theory are applied at score and decision level. The classification results are obtained using Support Vector Machine (SVM) classifier. In the last section, experimental results are provided and discussed.

Keywords: Inverse Synthetic Aperture Radar, Automatic Target Recognition, Edges detection and feature vectors, Information Fusion, Probability Theory, Majority Vote, Belief Theory.

(Received July 24, 2009 / Accepted December 03, 2009)

1 Introduction

Automatic Target Recognition (ATR) systems are an important part of modern military strategy. Correct recognition of military targets such as aircraft, naval ships, missiles etc, is indispensable to attack the target accurately. However, several kinds of radar signatures can be applied to acquire information about the target characteristics. Usually, these radar signatures deal with the extraction of certain geometrical parameters or characteristics of a target that can be obtained from a radar image such as Inverse Synthetic Aperture Radar (ISAR).

In this work, we present a radar information system for target recognition based on ISAR images. The methodology used in this framework is issued from artificial intelligence in following the Knowledge Discovery from Data (KDD) Process which has been adapted to radar field.

Generally, four steps are usually involved in automatic target recognition (ATR). They are data acquisition, data pre-processing, data representation and data classification for decision making.

However, with the KDD methodology applied to automatic target recognition, some details are given in the previous steps and another terminology is used: data ac-

quisition, data preparation, Data Mining (DM), and the evaluation and decision making step.

In the first step, data (signals) are collected and stored from an anechoic chamber which is used as a specific environment of experimentation. In this step each target is illuminated with a frequency stepped signal and the returned echoes are stored in the database. It is followed by the data preparation step which mainly includes data pre-processing and data transformation to decrease high dimensionality of signal and to increase the significant aspect of data raw visualization collected in step one. Hence, in the ATR framework, this step generally performs the reconstruction of ISAR images followed by attributes extraction. Thus, the attributes extraction are also called feature vectors which are used in the classification step in order to recognize unknown targets. Finnaly, the latest step is dedicated to evaluate and interpret the ATR results. These four steps are illustrated in figure 1.

Because of the large dimension of an ISAR image (Memory and complexity) and the information redundancy contained in pixel images, using directly the whole image for classification is inappropriate and can provide some errors in recognition task due to variations of illumination, scale and orientation, etc. For this reason and in order to reduce the dimensionality of ISAR image, we use features that are related to target shape geometry, such as moments and fractal dimension [5] applied on the shape target.

The presence of speckle noise [17] and the dark and light pixels in ISAR images complicates the extraction of target shape. However, several approaches of shape extraction from ISAR images have been proposed in the literature. The methods based on filters and convolutions produce an unclosed shape and the algorithm for closing it, is complex and takes a long computation time. Many others solutions have been proposed, such as watershed segmentation applied to ISAR image in [26] and the Gradient Vector Flow (GVF) [22] based on an Active Deformable Contours (ADC, known as Snakes). However, they present several limits. The first scheme produces an over-segmentation that requires a post-processing and the second method produces artifacts in the final contour and requires an initial contour geometry similar to the object edge. The drawbacks of this methods can be effectively avoided by using the approach that we proposed in [21]. This last one is based on combination of Smallest Univalue Segment Assimilating Nucleus (SUSAN) algorithm [25] and Level Sets method [4]. The idea is to exploit the distribution of dark and light pixels into the target area by modifying SUSAN algorithm and in order to classify the image pixels into two regions, the target region and the background region. Then, we apply a Variational of Level Sets (VLS) method to obtain a close target shape. We compared the effectiveness of this technique with other one used recently in radar field.

To guarantee scale and orientation invariance of shapes, Fourier Descriptors (FD) and Moment Invariants (MI) are used and then compared.

In second part of this paper, we focus on classification step. Recent researchs in ISAR image classification can be found in [18] [11]. The Radical Basic Function (RBF) based on Support Vector Machine (SVM) with one-against-one strategy is used. The classification systems based on one dimensional image (1D-image) such as Range Profile [19] provides a high performance than those based on radar images, in spite of the fact that the ISAR images show two dimensional (2-D) distribution of target. Indeed, it is often due to the insufficiency of a single feature to capture all of the classification information available in the pattern image. Thus, one of the solution for improving the ATR performance is finding and combining efficient and discriminative information about target shape that are invariant to geometrical transformations. So, we propose information fusion at two levels: (i) the feature level combined with concatenating MI and FD, (ii) and the classifier level fusion. At the classifier level, three fusion models have been investigated and compared: the rules based on the probabilities theory (Sum, Max, Min, Product, Median rules), the majority voting approach and belief approach. The main advantage of the two first models is their simplicity of implementation and for belief theory, its possibility to model the imprecision and uncertainty.

The remainder of this paper is organized as follows: section 2 present the methods used to extract feature vectors. Classifier fusion models are described in section 3. Section 4 is dedicated to evaluate and compare the performance of the proposed methods. Finally, in section 5, we conclure and give avenues for future work.

2 Image Preprocessing and feature extraction

2.1 ISAR Image Preprocessing

The ISAR image is usually affected by a multiplicative noise known as speckle [17] mainly due to the interference constructively or destructively of radar waves. These interferences produce light and dark pixels in ISAR image. This noise provides a poor quality of ISAR image and consequently, the interpretation of image and shape detection become difficult. Increasing the image quality and reducing speckle effect becomes a crucial

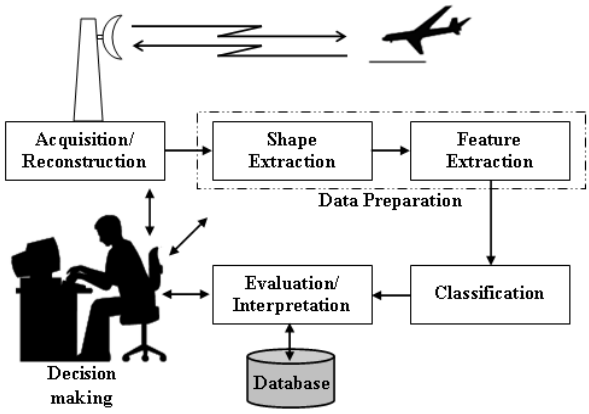

Figure 1: KDD process for Radar ATR system

process in our recognition system.

According to literature, there exist different filters able to reduce speckle, such as Kuan, Frost [8] and Lee [15]. We use synthetic data simulated in an anechoic chamber. So, speckle noise is not strong in the reconstructed images. Hence, we use a linear filter followed by median filter (see figure 4.b). The median filter can be replaced by Lee filter when the ISAR image is influenced by a strong speckle.

2.2 Target Shape Extraction

Several approachs for shape extraction have been proposed and tested such as filtring method (with Prewit filter), watershed segmentation and GVF methods. In this paper, we present another new method that gives us a satisfactory results. To make a visual human interpretation easier and guarantee a saisfactory calssification accuracy, we have proposed in [21] one approach that based on the combination of two methods: a modified SUSAN and a variational of Level Sets (VLS).

2.2.1 a modified SUSAN

The Smallest Univalue Segment Assimilating Nucleus (SUSAN) algorithm is introduced by S.M. Smith [25]. Usually, it's used for low level image processing; in particular, edge extraction, corner detection and noise reduction. SUSAN method has many differences to the others well known methods. The most obvious is that neither derivative image nor noise reduction is used or needed.

In this work, we view SUSAN operator like a preprocessing step and we have modified it in order to segment the ISAR image into two regions (the target region and the background region). We place a circular mask on each pixel of the input image, then we compute the sum S of gray level comparison between a mask center (Nucleus) and the others pixels within the local mask area (named also USAN) using the following equation:

$$S = \sum_{i \in USAN} exp\left\{ - \left(\frac{I(x_i, y_i) - I(x_0, y_0)}{t}^6 \right) \right\} \quad (1)$$

Where $I(x_0, y_0)$ and $I(x_i, y_i)$ correspond respectively to the gray level of nucleus and any pixel of mask area, t represents the threshold. Then, we classify the pixels according to three cases:

- If the concerned pixel has a gray level lower than the threshold fixed and located in an homogeneous area, the sum S of comparison will be large, because all gray scale levels of USAN pixels will be close to a nucleus gray level. Thus, the pixel is considered like a background.
- When the pixel has a gray level lower than the threshold and located in an heterogeneous area; if the sum S of comparison is greater than P/2 (P is the maximum value which can take the Sum S according to the mask size), we classify the pixel as a background, else it belongs to the object.
- If the pixel has a gray level higher than the threshold, then we classify the pixel in question like an object.

The difficulty of this technique comes from the choice of the threshold and the automation of this choice according to each ISAR image. However, we propose the threshold given by:

$$t = \frac{k}{MN} \sum_{i=1}^{M} \sum_{j=1}^{N} I(x_i, y_i) \quad (2)$$

Where M and N represent the dimension of ISAR image, and k is a natural constant that depends of image size to object size ratio.

We note that the circular mask used in this article contains 37 pixels with a radius of 3 pixels. Figure 4.c and figure 4.d present respectively the results of SUSAN and modified SUSAN methods applied on ISAR image.

2.2.2 Level Set

Level Set method is introduced by Osher and Sethian [20] for capturing moving fronts. It belongs to geometric active contours family and is based on Partial

Differential Equation (PDE) method. Level set presents several advantages over the traditional active contours. First, the topology changes automatically during curve evolution. Second, the level set can easily detect the concave boundaries and allows efficient numerical schemes.

The curve, denoted by C, is represented by the zero of a level set function $\phi(t,x,y)$:

$$C(t) = \{(x,y) \,|\phi(t,x,y) = 0\} \tag{3}$$

The evolution equation of the level set function ϕ which is called level set equation can be written in the following form:

$$\frac{\partial \phi}{\partial t} + F\,|\nabla \phi| = 0 \tag{4}$$

Where F is called the speed function and depends on the image data and the level set function ϕ.

We apply in this paper a variational formulation of level set method, which is computationally more efficient than the traditional level set methods. For more details about this variational and its numerical implementation, we invite the reader to see reference [16] and the references therein. The VLS method applied on Result of modified SUSAN and the results of other methods discussed above (Prewitt filter, watershed segmentation and GVF) can be shown in figure 4.

2.3 Shape Descriptors

Fourier descriptors (FD) [24] and moment invariants (MI) [7] belong respectively to two different families, algebraic invariants and integral invariants. FD and MI are widely used as shape features due to their good performance in recognition systems and their implementation simplicity and efficiency. They are invariant to almost all geometrical transformations such as translation, scaling and rotation.

2.3.1 Fourier Descriptors

Fourier descriptors represent the contour in the frequency spectrum. Low frequency coefficients describe the general information about the shape, whereas high frequency coefficients contain information about noise and details presented in the shape.

Let a contour coordinates be denoted by (x_i, y_i), $i = 1, 2, ..., L$ where L is the number of pixels in the contour. Many shape signature can be used as shown in [23, 26] and using the centroid distance outperforms the other shpe signatures in recognition and retreival purpose. The centroid distance vector r is defined as the distance between boundaries coordinates (x_i, y_i) and the center ,noted (x_c, y_c) of image.

$$r(i) = \left([x(i) - x_c]^2 + [y(i) - y_c]^2 \right)^{1/2} \tag{5}$$

Where $x_c = \frac{1}{L}\sum_{i=0}^{L-1} x(i)$, $y_c = \frac{1}{L}\sum_{i=0}^{L-1} y(i)$

Before applying the Fourier transform, all the shapes are normalized to 64 points ($L = 64$) in order to accomplish the recognition task. Finally, we obtain a Fourier descriptors using discrete Fourier transform on centroid distance vector:

$$FD_n = \frac{1}{L}\sum_{k=0}^{N-1} r(i) exp\left(\frac{-i2\pi nk}{L}\right), n = 0, 1, ..., L-1 \tag{6}$$

The FDs computed in this way are chosen in order to achieve the rotation invariance. The phase information of the FDs is ignored and only the magnitude $|FD|$ is used. Afterwards, we divide the magnitudes by the DC component, i.e. $|FD|$. Only half of the $|FD|$ is needed to index the shape target.

2.3.2 Moment Invariants

Let a binary image be denoted by $I(x,y)$,The $(p+q)^{th}$ order moment relative to the image are defined by:

$$m_{pq} = \sum_{x=1}^{M}\sum_{y=1}^{N} x^p y^q I(x,y) \tag{7}$$

Where M and N represent its dimension (M rows,N columns). This ordinary moment can not be directly applied like a shape descriptors because they are not invariant to several transformations (scale, rotation, translation, etc). Hence, we use the normalized central moments which are invariant to scale and translation. They are computed by:

$$\eta_{pq} = \frac{\mu_{pq}}{\mu_{00}^r}, r = 1 + (p+q)/2, p+q = 2, 3, ... \tag{8}$$

Where:

$$\mu_{pq} = \sum_{x=1}^{M}\sum_{y=1}^{N} \left(x - \frac{m_{10}}{m_{00}}\right)^p \left(y - \frac{m_{01}}{m_{00}}\right)^q I(x,y) \tag{9}$$

Basing on normalized central moment of second and third order, M. K. Hu [9] introduced a set of seven rotation invariant features. We present only four of them and the remaining coefficients can be found in [9].

$$\begin{aligned} \phi_1 &= \eta_{20} + \eta_{02} \\ \phi_2 &= (\eta_{20} + \eta_{02})^2 + 4\eta_{11}^2 \\ \phi_3 &= (\eta_{30} - 3\eta_{12})^2 + (3\eta_{21} - \eta_{03})^2 \\ \phi_4 &= (\eta_{30} - \eta_{12})^2 + (\eta_{21} - \eta_{03})^2 \end{aligned} \tag{10}$$

We note that the shape normalization is not needed in the case of moment invariants.

3 Information Fusion schemes

Usually, information fusion [1] can be carried out at four following levels:

- Sensor level fusion refers to the combination of raw data from different sensors.
- Feature level fusion refers to the combination of different features vector.
- Score level fusion refers to the combination of matching scores provided by different classifiers.
- Decision level fusion refers to the combination of decisions provided by individual classifiers.

In our work, we focus on three levels fusion: feature, score and decision level fusion. The first one is used by concatenating two different features vector extracted from the shapes (Fourier descriptors and moment invariants). The second and the third schemes are achieved respectively by combining the matching scores and decisions obtained by the three classifiers (FD based SVM,MI based SVM and FD-MI based SVM). Three fusion methods are investigated: the rules based on Probability approach (Product, sum, max, min and median rules) [13], majority vote rule [12] and belief theory (known as Dempster - Shafer) [14]. Many researchs of information fusion applied for target recognition in radar field can be showed in [6] [10].

3.1 Rules based on Probability approach

This approach proposes to combine the posterior probabilities offered by the individual classifiers. Considering M classifiers $\{S_1, ..., S_M\}$, C classes $\{w_1, ..., w_c\}$ and $P(w_c|X_j)$ the posteriori probability for a class w_c offered by classifier j for a feature input X_j. Several ways to implement the combination of these probabilities are then obtained:

- **Product rule:** $\max_{k=1,...,C} \prod_{j=1}^{M} P(w_k|X_j)$.
- **Sum rule:** $\max_{k=1,...,C} \sum_{j=1}^{M} P(w_k|X_j)$.
- **Max rule:** $\max_{k=1,...,C} \underset{j=1,...,M}{max} P(w_k|X_j)$.
- **Min rule:** $\max_{k=1,...,C} \underset{j=1,...,M}{min} P(w_k|X_j)$.
- **Median rule:** $\max_{k=1,...,C} \underset{j=1,...,M}{med} P(w_k|X_j)$.

3.2 Majority vote rule

The majority vote rule [12] is the simplest approach for fusion due to its simplicity of implementation. The class z most voted by the individual classifier is chosen by computing the number of times that each class appears:

$$z = \underset{k=1,...,C}{\operatorname{argmax}} \sum_{j=1}^{M} \alpha_j \, Q_{jk} \tag{11}$$

Where

$$Q_{jk} = \begin{cases} 1 & \text{if } p(w_k|X_j) = \max\limits_{i=1,...,C} P(w_i|X_j); \\ 0 & \text{otherwise.} \end{cases} \tag{12}$$

and

$$\sum_{j=1}^{M} \alpha_j = 1. \tag{13}$$

The coefficients α_j represent the reliability degree of classifiers and we can estimate them by using the recognition rate of each classifier. We use these coefficients to tackle the problem of the conflict between the classifiers.

3.3 Belief theory

The theory of belief functions known as Dempster-Shafer theory is an extension of the probabilities theory. The main advantage of this theory is the possibility to represent the imprecision and uncertainty. We propose here the use of belief theory for classifiers fusion.

Let Ω=$\{w_1, ..., w_c\}$ be a set of elements known as the frame of discernment (in our case, the set of class labels). The mass function m is defined over 2^Ω (the set of all subsets A of Ω) and represents the confidence degree of each subset A:

$$\begin{aligned} m : 2^\Omega &\longmapsto [0, 1] \\ A &\longmapsto m(A) \end{aligned}$$

With normalization condition, we have: $\sum\limits_{A \in 2^\Omega} m(A) = 1$.

Other belief functions can be defined from these mass functions, such as functions of credibility and functions of plausibility.

Estimating the mass functions is a difficult step of belief theory. Several models have been proposed in literature and their choice must be done according to the nature of data and application. Appriou [3] proposed two models based on three axioms. The first one involve the use of $C \times M$ mass functions associated to the focal elements $\{w_k\}$, $\{w_k^c\}$ and Ω and the second axiom limits the mass functions to two types. The third

one guarantees the equivalence with the probability approach where the reality is perfectly known. The two models are substantially equivalent for our data. So, we use in this work the model given by:

$$\begin{cases} m_{jk}\left(w_k\right)(X) = \frac{\alpha_{jk} R_j P(S_j|w_k)}{1+R_j P(S_j|w_k)} \\ m_{jk}\left(w_k^c\right)(X) = \frac{\alpha_{jk}}{1+R_j P(S_j|w_k)} \\ m_{jk}\left(\Omega\right)(X) = 1 + \alpha_{jk} \end{cases} \quad (14)$$

Where $R_j = \left(\max_{j,k} P(S_j|w_k)\right)^{-1}$ is a normalization factor, and $\alpha_{jk} \in [0,1]$ is a discounting coefficient that represents the reliability of information provided by the classifier S_j about the class w_k. In this work, we choose $\alpha_{jk} = 0.95$. The probabilities $P(S_j|w_k)$ can be estimated using confusion matrices obtained during the learning stage.

Combining $C \times M$ mass functions can be a real problem when this number is high. Several modes of combination have been proposed in literature. There exist two families: the conjunctive combination called also orthogonal sum and the disjunctive combination. The chosen model is proposed by Yager [27] and belongs to conjunctive combination model. Yager rule is defined for two mass functions m_1 and m_2 and for all $A \in 2^\Omega$ by:

$$\begin{cases} m\left(A\right) = m_{Conj}\left(A\right) \\ m\left(\Omega\right) = m_{Conj}\left(\Omega\right) + m_{Conj}\left(\emptyset\right) \end{cases} \quad (15)$$

$$\text{Where } m_{Conj}\left(A\right) = \sum_{B,C \in 2^\Omega, B \cap C = A} m_1\left(B\right) m_2\left(C\right) \quad (16)$$

$m_{Conj}\left(\emptyset\right)$ represent a non-expected solution.

The decision is the final step of the process. It is made one all the mass functions that have been combined into a single one m. Generally, we consider the maximum of one of the three functions: credibility (Pessimist criterion), plausibility (Optimist criterion) and pignistic probability. We choose in this work the criterion employing the pignistic probability which is the most used compromise. The pignistic probability is given for all $A \in 2^\Omega$, with $A \neq \emptyset$ by:

$$betP(A) = \sum_{B \in 2^\Omega, B \neq \emptyset} \frac{|A \cap B|}{|B|} \frac{m\left(B\right)}{1 - m\left(\emptyset\right)} \quad (17)$$

4 Experiment Results and comparison

4.1 Experiment setup

The radar data is simulated from an anechoic chamber of ENSIETA (Brest, France) in a specific environment of experimentation (Figure 2). We use seven targets (A10, Mig29, Harrier, F16, F117, Tornado, Rafale) in our experiment represented by aircraft scale reduced models (1/48) and are shown on Figure 3.

Figure 3: Scale reduced aircraft models used in the anechoic chamber

Each target is illuminated by a frequency stepped signal with a bandwidth B between 11.65 GHz and 18 GHz, and a frequency increment $\Delta f = 50$ MHz (128 frequency samples). 162 images of each target have been generated corresponding to 201 angular positions, from $-5°$ to $95°$ with an angular increment β = 0.5°. We obtained an ISAR image from the complex signature recorded over an angular sector of $\nabla\alpha = 20°$ with an angular increment β. Consequently, after data resampling and interpolation, the slant range and cross range resolution and ambiguity window are given by:

$$\begin{aligned} \Delta R_S &= \frac{c}{2B} \cong 2.4cm,\ W_S = \frac{c}{2\Delta f} \cong 3m \\ \Delta R_c &= \frac{\lambda}{2\nabla\alpha} \cong 2.9cm,\ W_c = \frac{\lambda}{2\Delta\alpha} \cong 1.16m \end{aligned}$$

The ISAR image represents spatial distribution of scattering centers, and can be produced by both azimuth and range analysis. Range analysis provides a range profile, and the resolution of differential Doppler caused by target rotation gives an orthogonal dimension (cross-range). The appropriate technique to construct ISAR images is the Inverse Fast Fourier Transform (IFFT) [26].

4.2 Experiment results

To evaluate the robustness of our approach used in recognition process, we have used 7 aircraft targets. Each target is represented by 162 ISAR images of 256×256 gray pixels, with different angle of view varying angle. The whole data set includes $162 \times 7 = 1134$ ISAR images. Two scenarios are used for testing, the first one is 10-fold cross-validation scenario. For the second one, The whole database is divided into two data sets, 100 images of each target (61%) are used to constrcut the training data and the remaining images are used for testing. From the shapes extracted using different methods

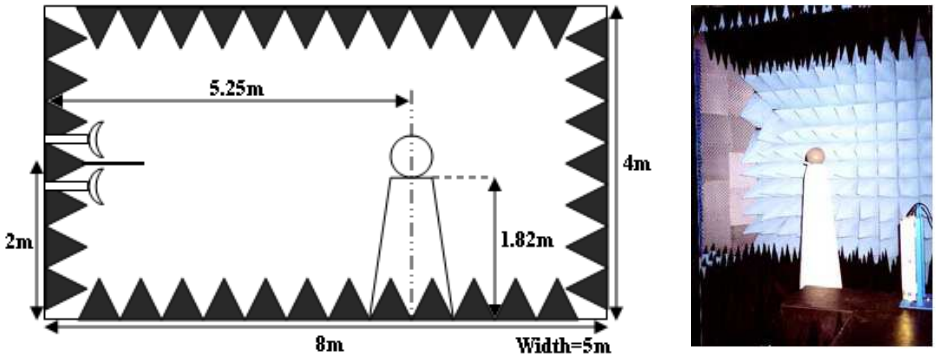

Figure 2: Anechoic chamber of ENSIETA

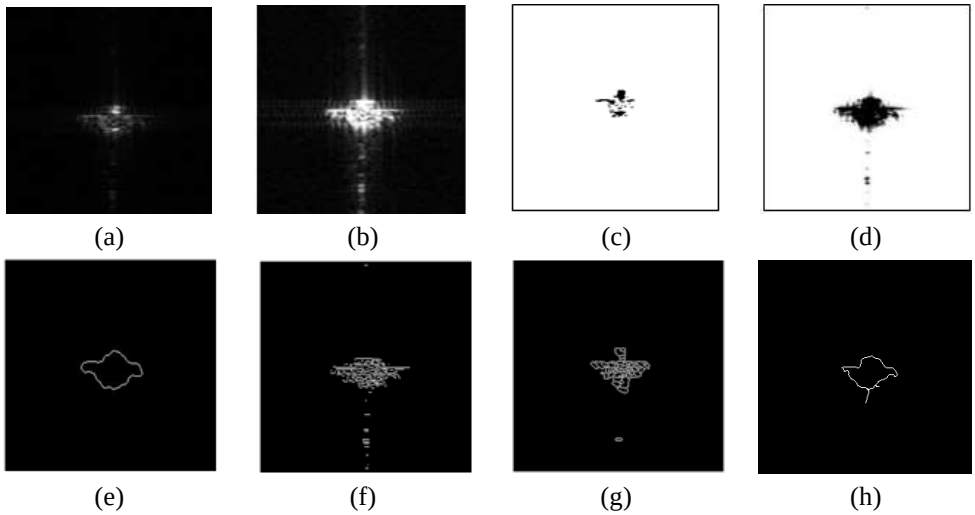

Figure 4: Results of image Preprocessing and shape extraction. (a) ISAR image OF Mig.29 ($5°$), (b) Image Preprocessed, (c) SUSAN Algorithm, (d) SUSAN modified, (e) VLS on SUSAN modified result, (f) Prewitt filter, (g) Watershed segmentation, (h) Gradient Vector Flow

(SUSAN+VLS, GVF, VLS, watershed), the Fourier descriptors (FD=31 descriptors) and the moment invariants (MI=7 coefficients) are computed. Therefore, the Principal Components Analysis (PCA) is applied on Fourier descriptor vector in the whole database in order to reduce the dimension of descriptors, As result, the template of Fourier descriptors contains only 20 Fourier descriptors. In absence of a ground truth and the insufficiency of the visual evaluation (figure 4) which shows that SUSAN algorithm followed by VLS method gives us the best result than the other methods, we use the correct rate of classification to evaluate and compare the methods of shape extraction. These results are obtained using an approach proposed recently in [2], Genetic Algorithms combined with Support Vector Machine (GA-SVM). The GA are used here to select the optimal Radical Basic Function (RBF) kernel parameter (c, γ) for SVM classifier. In the present work, the library LIB-SVM [1] was used. we note that this library implements the SVM with one-against-one voting terminology to handle more than two classes.

We present in table 1 and table 2 the recognition rates obtained using different techniques of shape extraction discussed above. We use in table 1 the 10-fold cross-validation scenario and in table 2 we present the results using the random partitioning of the whole database. The best result is obtained using our approach described in this paper with a recognition rates of 84.10% (random paritioning) and 87.24 %(10-fold cross-validation). On the other hand, the tables 1 and 2 show that the fusion of FD and MI provide a significantly better rate

[1] http://www.csie.ntu.edu.tw/ cjlin/libsvm

methods of shape extraction	Recognition rate (%)		
	FD	MI	FDMI
GVF	46.08%	48.12%	53.22%
VLS	67.28%	69.58%	75.11%
Watershed	56.45%	58.06%	60.36%
SUSAN+VLS	78.34%	81.33%	84.10%

Table 1: Classification rates according to techniques of shape extraction and feature vectors using the random partitioning scenario.

methods of shape extraction	Recognition rate (%)		
	FD	MI	FDMI
GVF	48.32%	50.79%	55.64%
VLS	68.69%	71.07%	76.80%
Watershed	58.28%	60.22%	63.93%
SUSAN+VLS	80.95%	83.86%	87.24%

Table 2: Classification rates according to techniques of shape extraction and feature vectors using the 10-fold cross-validation scenario.

than the individual features. We note also that the moment invariants are more robust than Fourier descriptors concerning the representation of the closed shapes.

Each SVM classifier FD based SVM, MI based SVM and FD-MI based SVM provides partial scores that determine the class of the input vector. These partial scores are then transformed into probabilities prior to combination. Several fusion techniques are tested, the rules based on probability theory (Product, Sum, Max, Min, Median rules), the majority vote rule and the belief theory. The results of these combination models are summarized in table 3.

		Recognition rates (%)
Probability theory	Product rule	86.63%
	Sum rule	86.63%
	Max rule	86.40%
	Min rule	85.48%
	Median rule	87.78%
Majority vote rule		87.78%
Belief theory		89.63%

Table 3: Classification rates of fusion models.

According to table 3, the results of fusion models show that it's possible to achieve a good fusion performance by carefully choosing the best fusion technique. We observe that belief approach provides a better recognition rate (89.63%) that other fusion models. Both approaches, majority voting and median rule, give similar classification rates (87.78%). We note also that during the classification operation, belief fusion apprach is more slower than the probability theory and the majority vote rule.

5 Conclusions and Perspectives

In this work, we have proposed a system for automatic target recognition based on a new approach for shape extraction. This approach is based on the combination of a modified version of SUSAN algorithm and VLS method. The results show that our method outperforms all the other methods in term of recognition rate. In the second part of this work, we have investigated the impact of information fusion on system performance according to three levels: the feature level, the score level and the decision level. We conducted an extensive classification experiments using RBF kernel based SVM classifier and a various classifier combination schemes such as rules based Probability theory (product, sum,...), majority vote and the belief theory. We observed that the combined classifiers improve the ATR performance of either alone when the best fusion rule is carefully selected. Despite the fact that the belief theory is complex in implementation, a combined classifier employing it provides the best classification results and produces the most reliable decisions. As a future work, we want to validate the results of shape extraction against the noisy ISAR images, and we want also to study other advanced combination schemes such as the possibility theory and naive bayes.

References

[1] Aguilar, J. F. Adapted fusion schemes for multimodal biometric authentication. *PhD thesis, UNIVERSIDAD POLITECNICA DE MADRID, Spain*, May 2006.

[2] Amine, A., el Akadi, A., Rziza, M., and Aboutajdine, D. Ga-svm and mutual information based frequency feature selection for face recognition. *Infocomp Journal of Computer Scienc*, 8(1):20–29, 2009.

[3] Appriou, A. Decision et reconnaissance des formes en signal. *Hermes Science Publication*, 2002.

[4] Ayed, I., Mitiche, A., and Belhadj, Z. Multiregion level-set partitioning of synthetic aperture radar images. *IEEE Transactions on Pattern Analysis and Machine Intelligence*, 27(5):793–800, 2005.

[5] Backes, A. R. and Bruno, O. M. Fractal and multiscale fractal dimension analysis: A comparative study of bouligand-minkowski method. *Infocomp Journal of Computer Science*, 7(2):74–83, June 2008.

[6] Buede, D. M. and Girardi, P. A target identification comparison of bayesian and Dempster-Shafer multisensor fusion. *IEEE Transactions on Systems, Man and Cybernetics, Part A: Systems and Humans*, 27(5):569–577, 1997.

[7] Flusser, J. and Suk, T. Rotation moment invariants for recognition of symmetric objects. *IEEE Transactions on Image Processing*, 15:3784–3790, 2006.

[8] Frost, V., Stiles, J., Shanmugan, K., and Holtzman, J. A model for radar images and its application to adaptive digital filtering for multiplicative noise. *IEEE Transactions on Pattern Analysis And Machine Intelligence*, 4(2):157–166, March 1982.

[9] Hu, M. K. Visual pattern recognition by moment invariants. *IRE Transactions Information Theory*, 32:179–187, 1962.

[10] Jouny, I. Target identification using multi-radar fusion. *Proc. SPIE*, 6566, 2007.

[11] Kim, K. T., Seo, D. K., and Kim, H. T. Efficient classification of ISAR images. *IEEE Transactions on Antennas and Propagations*, 53(5):1611–1621, 2005.

[12] Kuncheva, L. I. Switching between selection and fusion in combining classifiers: An experiment. *IEEE Transactions on systems, Man and Cybernetics*, 32(2):146–156, 2002.

[13] Kuncheva, L. I. A theoretical study on six classifier fusion strategies. *IEEE Transactions on Pattern Analysis and Machine Intelligence*, 24(2):281–286, 2002.

[14] Laanaya, H., Martin, A., Aboutajdine, D., and Khenchaf, A. Classifier fusion for post-classification of textured images. *Information Fusion, Cologne, Germany*, 2009.

[15] Lee, J. Speckle analysis and smoothing of synthetic aperture radar images. *Computer Graphics and Image Processing*, 17(1):24–32, September 1981.

[16] Li, C. M., Xu, C. Y., and Gui, C. F. Level set evolution without re-initialization: A new variational formulation. *IEEE International Conference on Computer Vision and Pattern Recognition, San diego, CA, USA*, June 2005.

[17] Lopez-Martinez, C. and Fabregas, X. Polarimetric sar speckle noise model. *IEEE Transactions on Geoscience and Remote Sensing*, 41(10):2232–2242, October 2003.

[18] Martorella, M., Giusti, E., Berizzi, F., and Mese, E. D. Automatic target recognition of terrestrial vehicules based on polarimetric ISAR image and model matching. *International Radar Conference, Adelaise, Australia*, 2008.

[19] null Jeng-Kuang Hwang, null Kun-Yo Lin, null Yu-Lun Chiu, and null Juinn-Horng Deng. Automatic target recognition based on high-resolution range profiles with unknown circular range shift. *IEEE International Symposium on Signal Processing and Information Technology*, pages 283–288, 2006.

[20] Osher, S. and Sethian, J. A. Fronts propagating with curvature dependent speed: algorithms based on Hamilton-Jacobi formulations. *Journal of Computer Physics*, 79:12–49, 1988.

[21] Saidi, M., Daoudi, K., Khenchaf, A., Hoeltzener, B., and Aboutajdine, D. Automatic target recognition of aircraft models based on ISAR images. *IEEE International Geoscience and Remote Sensing Symposium, IGARSS, Cape Town, South Africa*, 2009.

[22] Saidi, M., Toumi, A., Hoeltzener, B., Khenchaf, A., and Aboutajdine, D. ISAR data dynamics: target shapes features extraction for the design. *7th european conference on synthetic aperture radar, EUSAR, Friedrichshafen, Germany*, 2008.

[23] Saidi, M. N., Hoeltzener, B., Toumi, A., Khenchaf, A., and Aboutajdine, D. Automatic recognition of ISAR images: Target shapes features extraction. *International Conference on Information and Communication Technologies: from Theory to Applications, Damascus, Syrie*, 2008.

[24] Sarfraz, M. Object recognition using fourier descriptors: Some experiments and observations. *International Conference on Computer Graphics, Imaging and Visualisation*, 2006.

[25] Smith, S. and Brady, J. M. Susan: A new approach to low level image processing. *International Journal of Computer Vision*, 23(1):45–78, 1995.

[26] Toumi, A., Hoeltzener, B., and Khenchaf, A. Hierarchical segmentation on ISAR image for target recongition. *International Journal of Computational research*, 5:63–71, 2009.

[27] Yager, R. On the Dempster-Shafer framework and new combination rules. *Informations Sciences*, 41:93–137, 1987.